

Miraging a Majorana

P. D. Sacramento^{1,2,*}

1 CeFEMA, Instituto Superior Técnico, Universidade de Lisboa, Av. Rovisco Pais, 1049-001
Lisboa, Portugal

2 Beijing Computational Science Research Center, Beijing 100193, China

* pdss@cefema.tecnico.ulisboa.pt

March 10, 2024

Abstract

The image of a Majorana mode located on the focus of an elliptical corral of free electrons is studied. The Majorana mode may be taken at the edge of a topological wire superimposed on the two-dimensional electron gas. At low energies the states of the wire are ignored except for the Majorana mode. Usual tunneling to a fermionic mode is compared. In the favorable cases, tunneling to a Majorana mode leads to an enhanced mirage effect and a spectral weight mainly confined around the foci, in comparison to the tunneling to a fermionic mode. The Majorana character of the image is shown computing the self-conjugacy.

Contents

1	Introduction	2
2	Local impurity in elliptical corral	4
3	Hybridization to wire edge: fermionic vs. Majorana modes	5
3.1	Local density of states	7
3.2	Differential density of states	10
4	Two wires	11
5	Conclusions	11
6	Acknowledgements	12
A	Hamiltonian matrix	13
	References	14

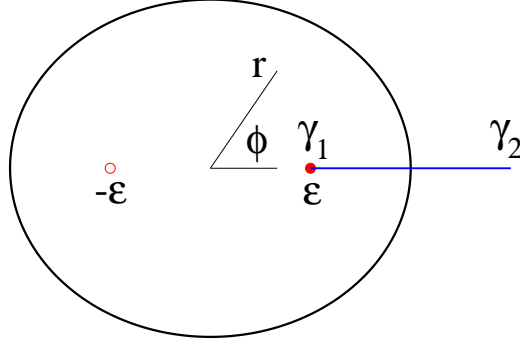


Figure 1: (Color online) Elliptical corral and wire with Majorana modes at the edges.

1 Introduction

Waves in confined geometries have complex interference patterns. An interesting example is the enhanced image amplitude at one focus of some confined geometry [1,2], like elliptical [3,4], parabolic [5,6] or stadium corrals, of some state with significant amplitude at the other focus. This phenomenon has been named the mirage of a state. Examples in quantum mechanical systems have been found both theoretically and experimentally such as the image of a Kondo resonance [7–9], an impurity located at one of the foci [10,11], a magnetic impurity on a conventional superconductor [12–14]. Here we consider the corresponding situation of a Majorana mode placed at one focus of an elliptical corral and study how it affects the electronic density of states of a system of free fermions and how the information of this localized state is seen at the other focus.

The problem of a Majorana fermion interacting with free electrons has attracted attention, as a mean to its detection through the tunneling to and from the localized mode [15–17], since it has been shown that there is non-vanishing tunneling [18]. Another interesting aspect is the possibility to show, detect and use its intrinsic non-locality [19–22], since Majoranas appear in pairs and form highly non-local regular fermions and, therefore, may be used in long-distance teleportation [23–25]. The study of interference patterns on the surface of a topological insulator has also been considered recently [26], as have the mirages created by Andreev reflected states [27]. Also, the non-abelian character and robustness due to topological protection of Majorana modes, seems to offer a potentially useful way to implement topological quantum computation [28,29]. The braiding of the Majorana modes and, in general, their manipulation, has attracted considerable attention [30–32]. One example has been the manipulation of Majorana modes in structures involving collections of topological wires, for instance applying external fields that change the topological nature [33], such as pairing or chemical potential profiles, for instance using shuttles that carry Majorana modes as some domain wall is displaced along some wire [34]. The manipulation of the modes typically involves decoherence, such as due to quasiparticle poisoning, which is particularly

serious if the manipulation of the Majorana modes is not carried out slow enough, and requires some error correction, also due to some thermal noise [35–37]. However, the manipulation of the Majorana modes has been proposed to provide a way to establish networks for quantum communication [38] at arbitrary distances. The possible existence of a mirage of a Majorana mode may lead to the possibility of manipulation of the Majorana modes without transport, and may offer a way to avoid or decrease the decoherence, with a transmission of information through the states in the corral. In this work we consider the conditions for its appearance.

The Majorana mode may arise in different situations such as at the ends of some topological wire. Examples are semiconductor wires with spin-orbit coupling proximity coupled to a conventional superconductor and in the presence of some Zeeman term [39–41], or chains of magnetic impurities on top of a conventional or triplet superconductor, either forming some magnetic spiral order or ferromagnetically aligned with the extra effect of spin-orbit coupling, or even other orderings [42–46]. One possible system to study would be to consider a two-dimensional conventional superconductor with spin-orbit coupling, placing a ferromagnetically ordered long chain of magnetic impurities on top of the superconductor, such that one of its ends is placed on one of the foci of a corral. The corral may be implemented as in the study of a single impurity at the focus [12] placing a series of potential scattering impurities along an ellipse. Since the magnetic chain has to be sufficiently long so that the edge states do not overlap significantly and the edge modes have vanishing energies, the system to be studied is large and numerically expensive. It is therefore easier to analyse a situation in the continuum as represented in Fig. 1. We consider a system of electrons with a parabolic band in the confined geometry of an elliptical corral, implemented imposing open boundary conditions, in interaction with a wire that is assumed to support some Majorana mode at its edges. One of the edges is outside the corral and assumed far enough and, since we are interested in the low-energy properties, we assume the wire can be simulated exclusively by the Majorana mode, γ_1 , located at the edge inside the corral.

The problem of free fermions can be solved exactly. One way is to use Mathieu functions [3]. Here we adopt, for simplicity, a description in terms of cylindrical Bessel functions. These are the solutions for a circular corral, in which case the two foci coincide. Introducing the eccentricity of the ellipse the Bessel functions are no longer eigenfunctions, but one can construct an Hamiltonian matrix which is tridiagonal, if we use properly rescaled variables [47]. Specifically, let us define the cartesian coordinates in a two-dimensional system as $x/a = r \cos(\varphi)$, $y/b = r \sin(\varphi)$. Here a and b are the major and minor axis of the ellipse, r is a radial coordinate and φ the angular coordinate. Given the eccentricity of the ellipse, ϵ , the distance of the foci to the origin is $f = a\epsilon$, and $\sigma = b/a = \sqrt{1 - \epsilon^2}$. We will consider the case of $\epsilon = 1/2$. We solve Laplace's equation using the basis of the circular problem [4, 47]. We consider the basis of normalized states $\Phi_{k,n} = \langle \vec{r} | kn \rangle = R_{kn} J_k(\gamma_{kn} r) e^{ik\varphi}$. The function J_k is the cylindrical Bessel function of order k , R_{kn} ensure that the basis is orthonormalized and γ_{kn} is the n zero of the Bessel function of order k . Details of the method are presented in the appendix. The solution of the free electron problem in the elliptical geometry allows to identify states that have significant amplitudes at both foci, as required to obtain a significant mirage effect.

In section 2 the case of a simple potential impurity is briefly reviewed and the local density of states is calculated. In section 3 the tunneling to a fermionic or a Majorana mode at the edge of a wire superimposed on the elliptical corral is considered. The local density of states (LDOS), differential LDOS, and the self-conjugacy of the lowest energy modes are calculated, showing the enhanced mirage effect and Majorana character of the image at the other focus.

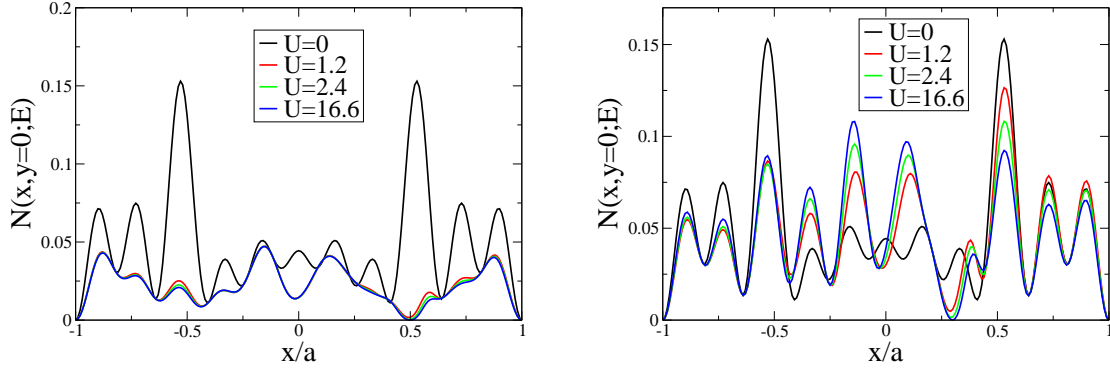


Figure 2: (Color online) Local density of states of a corral with a potential impurity, U , located at a) right focus and b) off focus. The energy E is chosen such that the density of states is high at both foci when the impurity is absent, $U = 0$.

In section 4 the case of two wires superimposed on the corral, with one edge at one or the other focus, shows the Majorana character at both wires, provided there is a Majorana mode in one of them. In section 5 the conclusions are presented.

2 Local impurity in elliptical corral

Let us consider first a two-dimensional system of free electrons in the presence of the corral without the wire, but with one impurity added [10] at site \vec{r}_i described by an Hamiltonian

$$H = \int d^2r c^\dagger(\vec{r}) \left(-\frac{\hbar^2}{2m} \nabla^2 \right) c(\vec{r}) + U \int d^2r \delta(\vec{r} - \vec{r}_i) c^\dagger(\vec{r}) c(\vec{r}) \quad (1)$$

Diagonalizing the Hamiltonian in the basis of Bessel functions, one may calculate the local density of states in the corral. The LDOS at point \vec{r} and energy E may be obtained as

$$N(\vec{r}, E) = \frac{1}{\pi} \sum_j \psi_j(\vec{r}) \psi_j^*(\vec{r}) \frac{\delta}{(E - E_j)^2 + \delta^2} \quad (2)$$

where $\psi_j(\vec{r})$ are the eigenstates, E_j the energy eigenvalues and δ is of the order of the lowest energy of the free problem, $U = 0$. The energy E is selected at a given E_j such that its wave function has a large amplitude at the foci locations [48].

In Fig. 2 we place the impurity at the focus $\vec{r}_i = (r = 1/2, \varphi = 0)$ or the impurity off focus at $\vec{r}_i = (r = 0.3, \varphi = 0)$. The effect of the repulsive potential at the impurity location is to reduce the LDOS. This is seen both when the impurity is placed on focus or off focus. The effect is clearly enhanced as the impurity strength, U , increases, but even a moderate impurity potential significantly reduces the density of states at the right focus. Both figures are obtained for the density of states calculated at an energy, E , that is such that, when the impurity is absent, there is a high spectral weight at both foci of the ellipse. As shown before,

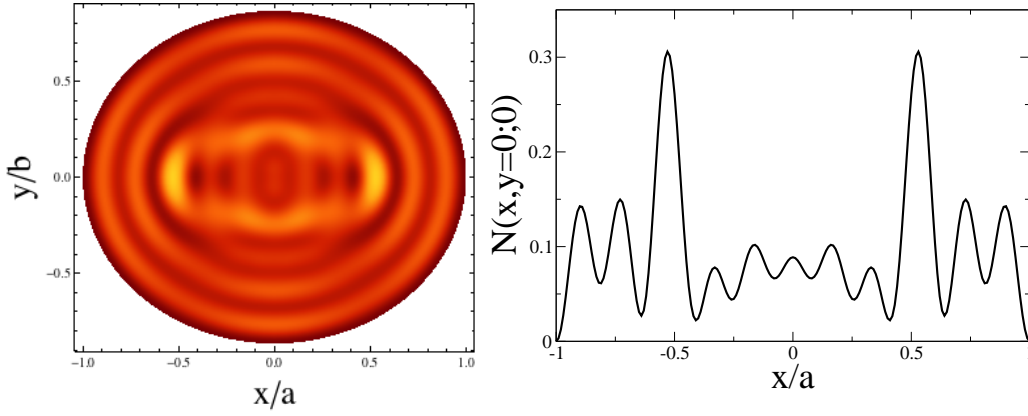


Figure 3: (Color online) Conduction electron contribution to a) two-dimensional local density of states with a chemical potential chosen at the energy, E , of Fig. 2 with the wire uncoupled, $t = 0, t_M = 0$. The lighter color corresponds to the larger density of states. b) A cut along the major axis of the ellipse.

this is essential to have a strong mirage effect. In Fig. 2 the mirage effect may be understood by the decrease of the density of states at $x = -\epsilon, y = 0$ due to the potential. Note that the mirage is not perfect even though the impurity potential is large. Placing the impurity off focus at $r = 0.3$, no such decrease of the density of states is observed at $x = -0.3, y = 0$. Indeed there is an anti-mirage effect [10], in the sense that the density of states is larger than that in the absence of the impurity. This different behavior highlights the significance of the mirage effect of the focus location.

3 Hybridization to wire edge: fermionic vs. Majorana modes

Let us now consider the situation with the wire in contact with the two-dimensional fermionic gas, with its edge located at \vec{r}_e and with no impurity present. The two edge Majorana modes couple to form a regular fermion as $d = 1/2(\gamma_1 + i\gamma_2)$. We consider now an Hamiltonian of the form

$$\begin{aligned}
 H &= \int d^2r c^\dagger(\vec{r}) \left(-\frac{\hbar^2}{2m} \nabla^2 - \mu \right) c(\vec{r}) \\
 &+ \int d^2r \delta(\vec{r} - \vec{r}_e) t \left(d + d^\dagger \right) \left(c(\vec{r}) - c^\dagger(\vec{r}) \right) \\
 &+ \xi_R \left(2d^\dagger d - 1 \right)
 \end{aligned} \tag{3}$$

The term that couples the electrons in the two-dimensional system with the Majorana mode at the edge of the wire may be expanded as

$$t \left(d + d^\dagger \right) \left(c(\vec{r}) - c^\dagger(\vec{r}) \right) \rightarrow t \left(c^\dagger d + d^\dagger c \right) + t_M \left(dc + c^\dagger d^\dagger \right) \tag{4}$$

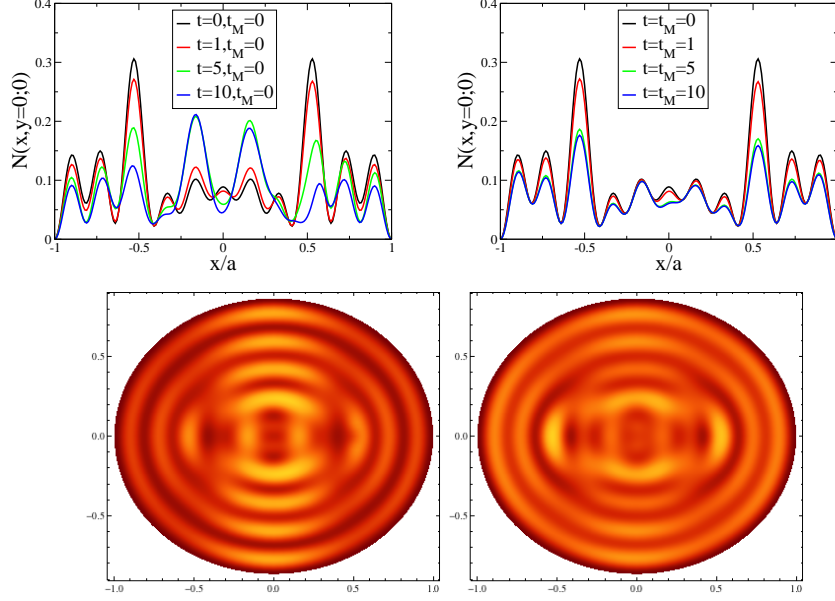


Figure 4: (Color online) Conduction electron contribution to the local density of states for a cut along the major axis in the case that the edge of the wire is placed at the right focus for a) a fermionic mode at the edge $t_M = 0$ and $t = 0, 1, 5, 10$ and b) a Majorana mode at the edge $t = t_M = 0, 1, 5, 10$. Two-dimensional local density of states with the edge of the wire placed at the right focus for c) a fermionic mode at the edge $t = 5, t_M = 0$ and d) a Majorana mode at the edge $t = t_M = 5$. The axis are as in Fig. 3.

The first term is the usual hopping to the edge of the wire. In the case of a Majorana $t = t_M$. Varying t_M we may tune the mode from a Majorana to a usual tunneling between regular fermionic states, obtained when $t_M = 0$. ξ_R is the exponentially small coupling between the two edges of the wire and μ is the chemical potential.

We may diagonalize the problem and determine the wave functions. These may be calculated expanding the wave functions of the electrons on the ellipse as

$$\begin{aligned} u(r, \varphi) &= \sum_{kn} u_{kn} \Phi_{kn}(r, \varphi) \\ v(r, \varphi) &= \sum_{kn} v_{kn} \Phi_{kn}(r, \varphi) \end{aligned} \quad (5)$$

In addition there is a state localized at the edge of the wire, characterized by the wave functions u_d and v_d .

Introducing the vector $\psi = (u_{kn}, u_d, v_{kn}, v_d)^T$, we may write the Hamiltonian matrix as

$$\begin{pmatrix} (H_0)_{k',n';k,n} & t\Phi_{k',n'}^e & 0 & t_M\Phi_{k',n'}^e \\ t\Phi_{k,n}^e & 2\xi_R & -t_M\Phi_{k,n}^e & 0 \\ 0 & -t_M\Phi_{k',n'}^e & -(H_0)_{k',n';k,n} & -t\Phi_{k',n'}^e \\ t_M\Phi_{k,n}^e & 0 & -t\Phi_{k,n}^e & -2\xi_R \end{pmatrix} \quad (6)$$

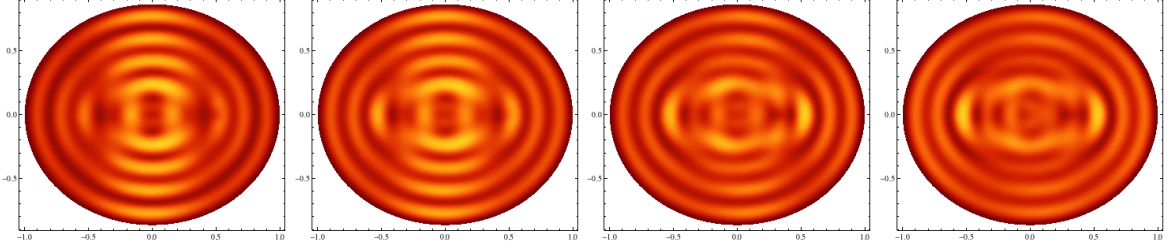


Figure 5: (Color online) In the two left panels the local density of states is shown taking μ between two energy levels, for $t = 5, t_M = 0$ and $t = t_M = 5$, respectively. In the two right panels μ is located at the energy level, E , but the wire edge is now placed off-focus. The same tunneling amplitudes are considered, respectively. The axis are as in Fig. 3.

Here $(H_0)_{k',n';k,n}$ is the matrix element in the Bessel function basis of $-\hbar^2/(2m)\nabla^2 - \mu$. Also, $\Phi_{k,n}^e$ is the basis function at the edge location, $\vec{r} = \vec{r}_e$, which may coincide with one focus or can be placed off-focus. We use energy units such that $\hbar^2/(2ma^2\sigma^2) = 1$. In these units the lowest energy is of the order of γ_{01}^2 , square of the first zero of the Bessel function of order 0.

3.1 Local density of states

Having solved the problem we may now calculate the LDOS in the corral. This can be obtained using

$$\begin{aligned}
 N(\vec{r}, \omega) &= \frac{1}{\pi} \sum_j \frac{\delta}{(\omega - E_j)^2 + \delta^2} (|u_j(r, \varphi)|^2 + \delta(\vec{r} - \vec{r}_e)|u_d|^2) \\
 &+ \frac{1}{\pi} \sum_j \frac{\delta}{(\omega + E_j)^2 + \delta^2} (|v_j(r, \varphi)|^2 + \delta(\vec{r} - \vec{r}_e)|v_d|^2)
 \end{aligned} \tag{7}$$

The energies, ω, E_j , are now measured with respect to the chemical potential. There are two contributions to the LDOS one coming from the conduction electrons in the corral and the other from the localized state at the edge location. In most results shown ahead we will present results for the LDOS of the conduction electrons.

In Fig. 3 we present results for conduction electron contribution to the LDOS with the chemical potential taken as $\mu = E$, for a cut along x . This corresponds to the case of Fig. 2 with no impurity, $U = 0$.

Let us now include the coupling between the wire and the electrons in the corral. In Fig. 4 we consider the edge of the wire at the right focus and compare the tunneling to a fermionic mode with the tunneling to a Majorana mode, as a function of the tunneling amplitudes. At the foci the effect is to reduce the density of states, in increasing rate as the tunneling amplitude increases. In the case of the tunneling to a fermionic mode the LDOS increases in the region near the center of the ellipse while tunneling to a Majorana mode this amplitude decreases with respect to the uncoupled wire. The character of the state of a large amplitude at the foci and small in between is preserved in the case of the tunneling to a Majorana. This behavior is clearly shown in Fig. 4 where the full two-dimensional local density of states is shown: the pattern of the tunneling to a Majorana mode displays the peaks at both foci while

the tunneling to a fermionic mode shows a spreading of the density of states over the corral and the mirage effect is lost.

The results shown so far were obtained fixing the chemical potential at a given eigenstate of the system with no wire and no impurity, specifically the level considered in Fig. 2 and placing the edge of the wire on the right focus. In Fig. 5 we calculate the LDOS taking the chemical potential between the state with energy E , considered above, and the next energy level of the free system. In the case of the tunneling to a fermionic mode, there is a decreased density of states at the foci and a considerable distribution along the smaller axis of the ellipse. On the other hand, in the case of tunneling to the Majorana mode, while there is still a large density of states at the foci, there is also a large density of states along the smaller axis and the character of the peaks centered at the foci is somewhat lost. In the same figure we also consider the density of states when the edge of the wire is off-focus and pinning again the chemical potential at the energy level of Fig. 2. We find that in the case of tunneling to a fermionic mode or a Majorana mode, the results are somewhat similar and the density of states does not change appreciably from the uncoupled wire case. A similar result is found if we pin the chemical potential to some energy level of the free system such that its wavefunction is not significantly peaked at the foci. In these cases the influence of the extra state at the edge of the wire is not very strong and the wavefunctions/density of states are not appreciably changed. This occurs also if the wire is placed off-focus. Therefore the mirage effect requires some fine tuning, as expected.

Taking into account the coupling between the two Majorana modes at the two edges of the wire (γ_1 and γ_2 in Fig. 1), which implies taking $\xi_R \neq 0$ does not change qualitatively the results, if the chemical potential is pinned at the same energy level. However, shifting the chemical potential between this level and the next, has the effect that the mirage effect is lost and the density of states is similar to the coupling to a fermionic mode. If the chemical potential is pinned between two free energy levels, even though there is a coupling to a Majorana-like mode (in the sense that $t = t_M$) the Majorana character is lost, since the two Majoranas of the wire are coupled and there is a gap in the spectrum. However, even if $\xi_R \neq 0$ but the chemical potential is pinned on one free energy level, there is a zero energy mode in the spectrum. However, this zero energy mode is not a true Majorana since the lowest state is not self-conjugate.

Further differences between the tunneling to a fermionic or to a Majorana mode are clearly seen in the density of states obtained integrating over space the LDOS. In the case of tunneling to a fermionic mode there is a gap in the energy spectrum while in the case of tunneling to a Majorana mode there is a zero energy mode. The effect of the tunneling to the Majorana edge state is better understood looking at the self-conjugacy of the wave functions indicative of a Majorana state. Considering a tunneling with $t_M = 0$, the Majorana character of the d mode is destroyed while if $t_M = t$ it is preserved, $|u_d|^2 - |v_d|^2 = 0$. The same test can be performed calculating at each point along x the quantity $\eta(r, \varphi) = |u(r, \varphi)|^2 - |v(r, \varphi)|^2$. Considering both cases the lowest energy eigenstate has a different structure. Specifically, when tunneling to a Majorana edge state the wave function of the lowest state is self-conjugate accross the corral. Moreover, while in the case of the fermionic mode tunneling the wave function has a significant amplitude accross the corral, in the case of the tunneling to a Majorana mode the wave function is strongly peaked at the focus location. These results are shown in Fig. 6. Note that the wave functions include a contribution from the local state at the right focus. Indeed, in the case of a Majorana mode this local mode contributes significantly with a sharp peak, as seen in the bottom right panel.

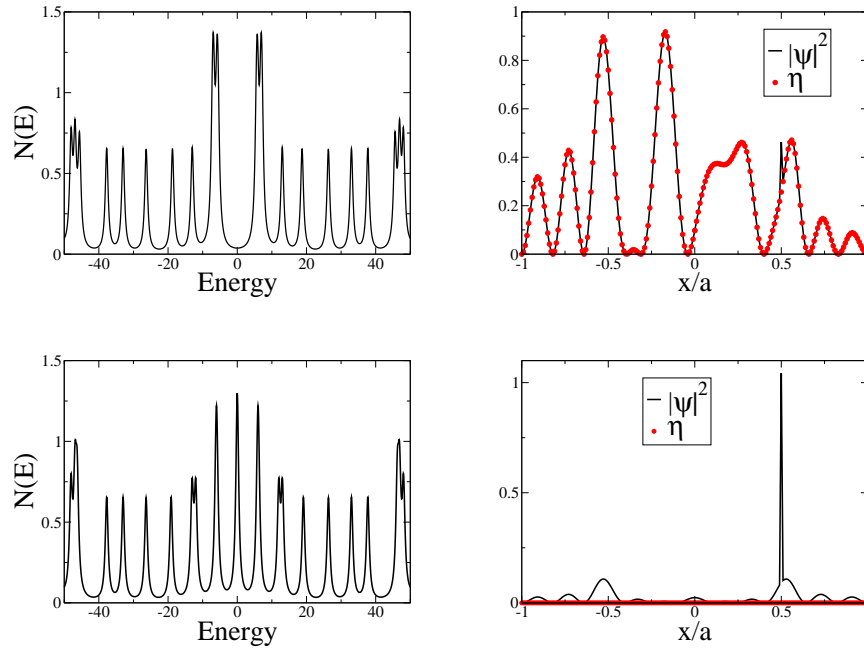


Figure 6: (Color online) Density of states (integrated over space) and self-conjugacy of the lowest energy state for the edge of the wire placed at the right focus for (top panels) a fermionic mode at the edge with $t = 5, t_M = 0$ and (bottom panels) a Majorana mode at the edge with $t = t_M = 5$.

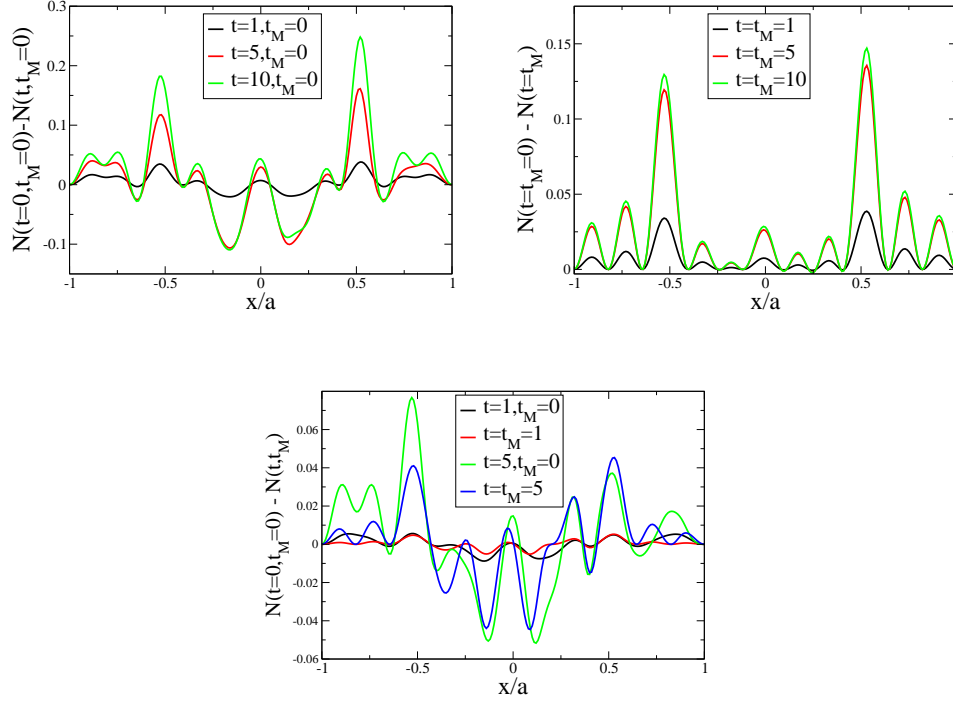


Figure 7: (Color online) Conduction electron contribution to the differential local density of states for a) a fermionic mode and b) a Majorana mode on focus, and c) both modes when the wire is placed off-focus.

3.2 Differential density of states

The effect of the hybridization to a local mode, either of fermionic or Majorana character, is better seen calculating the differential local density of states. The differential local density of states is defined by the difference between the LDOS of the uncoupled wire to the LDOS when the wire is hybridized with the conduction electrons.

In Fig. 7 the differential local density of states is compared, for the cases of the edge of the wire placed at the focus, for a fermionic and a Majorana mode. Also, the case of the local mode off focus is considered. In the case the edge is at the focus, as the tunneling increases the LDOS of the conduction electrons decreases in the neighborhood of the foci, both for a fermionic and a Majorana mode, as noticed in the previous subsection, and the differential LDOS increases significantly showing a pronounced mirage effect. However, as referred above and made clear by the differential LDOS, the effect in regions away from the foci is clearly different comparing a fermionic with a Majorana mode. In the case of the Majorana mode the change in the region between the foci is small while in the case of the fermionic mode there is a clear anti-mirage effect. In the case of a wire edge placed off-focus there is no clear mirage effect for either type of modes.

4 Two wires

The existence of the Majorana mode at the edge of the right wire may be detected introducing a second wire in the system. Consider the situation where we have one wire with one edge at the right focus and another wire with one edge at the other focus. We may now allow the tunnelings between the free electrons and the states at the wires to be either through a fermionic or a Majorana mode.

In Fig. 8 a few cases are considered, since one may tune either wire in or out of a topological phase or keeping both in trivial or topological phases. We plot the full LDOS in the two-dimensional corral (including both the conduction electron and local mode contributions), the lowest energy eigenfunctions and their self-conjugacies. In the left and right panels there is reflection symmetry and the groundstate is degenerate. If there are fermionic modes at the edges of both wires ($t_R = 5, t_M^R = 0, t^L = 5, t_M^L = 0$) the groundstate is symmetric around the center of the ellipse. However, if there are Majorana modes, even if the tunnelings are symmetric ($t^R = t_M^R = 5, t^L = t_M^L = 5$), the two wires couple and one of the wavefunctions in the lowest energy subspace of approximately zero energy is not symmetric. However, summing the contribution from the wave functions with zero energy symmetry is recovered. If both at the right and left foci there is a fermionic mode, the behavior just reflects the absence of a mirage and a high density of states in the central region of the ellipse. Also, the lowest energy state is peaked at foci but it is not self-conjugate. On the other hand if one of the two edge states is a Majorana, the lowest energy state has a Majorana character (self-conjugate). The most interesting case is when both edge states are Majoranas: there is the mirage effect mentioned above, the lowest state wavefunction is peaked at the foci and the mode is self-conjugate.

5 Conclusions

In summary, the tunneling between a free electron gas confined in an elliptical corral and a topological wire with a Majorana mode placed at one focus, leads to a mirage effect at the other focus, given the appropriate conditions. A condition common to all mirage problems implies that the chemical potential should be located on an energy eigenstate with a significant amplitude at the two foci. The effect of the coupling to the Majorana mode at the focus location, is to reduce the density of states in its vicinity, with a peak at its exact location, and maintaining a reduced density of states elsewhere in the corral. In the case of tunneling to a fermionic mode the mirage effect is lost, in the sense that there is an anti-mirage effect, since the density of states in the central region of the corral is enhanced with respect to the free system. The results show that the choice of the chemical potential is relevant since placing the chemical potential on an energy level that does not have a high amplitude on both foci, reduces the effect of the state at the wire edge. Also, placing the wire off-focus has a reduced effect for the same reason. The wave function of the Majorana mode, while mainly localized at the focus, extends throughout the corral maintaining its self-conjugacy. The difference between a coupling to a fermionic mode and a Majorana mode is enhanced calculating the differential local density of states. Also, the mirage effect is clearly seen in the case of placing the edge of the wire at one focus, instead of off focus.

Superimposing two wires on the two-dimensional system and placing the edges of each

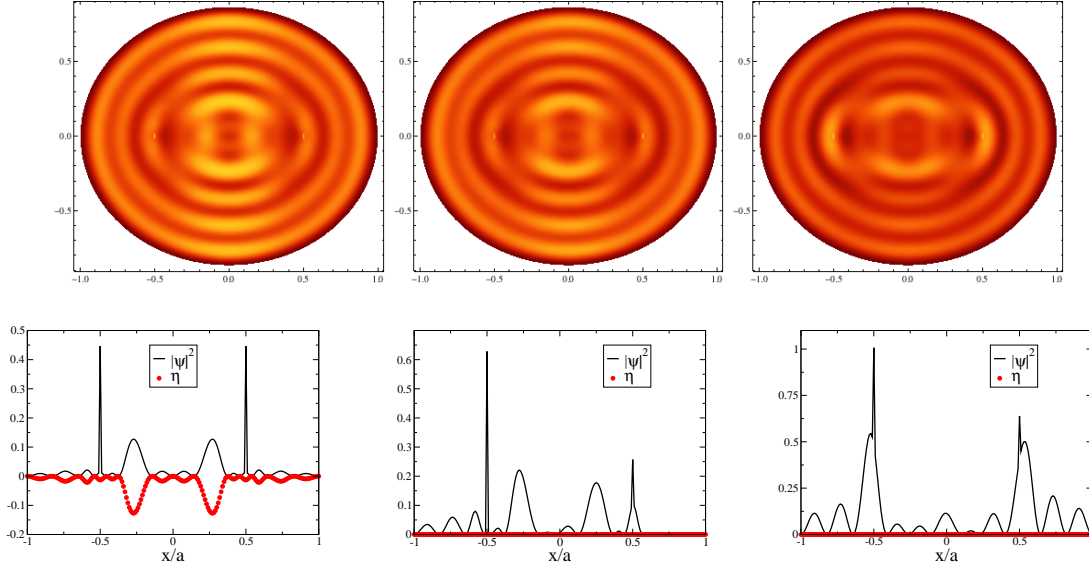


Figure 8: (Color online) Two wires at the foci: density of states, lowest energy eigenstate amplitude and self-conjugacy for $(t^R = 5, t_M^R = 0; t^L = 5, t_M^L = 0)$, $(t^R = t_M^R = 5; t^L = 5, t_M^L = 0)$, and $(t^R = t_M^R = 5; t^L = t_M^L = 5)$, respectively. In the case of the Majorana modes, the wavefunction is one of a degenerate set of solutions. The axis in the top panels are as in Fig. 3.

wire at the foci, leads to a mirage effect if both edge modes have a Majorana character but an extended mode with self-conjugacy is observed if at least one of the wires is in a topological phase with one edge Majorana.

The mirage effect may allow the teleportation of the Majorana character at arbitrary distances and one may imagine a network of wires that may interact non-locally. Tuning either one or both wires through a topological transition, it will be interesting to attest the transmission of information using the non-locality of the coupling between the Majorana modes. Acting locally on a Majorana mode, such as in Fig. 1 the right γ_2 Majorana, may affect the left edge of a second wire placed on the left focus, since Majoranas occur in pairs. The dynamics, response time and possible loss of coherence will be interesting to study.

6 Acknowledgements

Discussions with Pedro Ribeiro are acknowledged. Partial support from FCT through grant UID/CTM/04540/2013 is also acknowledged.

A Hamiltonian matrix

The Laplacian may be written as

$$\begin{aligned}
\nabla^2 &= \frac{\partial^2}{\partial x^2} + \frac{\partial^2}{\partial y^2} \\
&= f_r(\varphi) \frac{\partial^2}{\partial r^2} + f_\varphi(\varphi) \left(\frac{1}{r} \frac{\partial}{\partial r} + \frac{1}{r^2} \frac{\partial^2}{\partial \varphi^2} \right) + \\
&+ f_{r\varphi}(\varphi) \left(\frac{1}{r} \frac{\partial^2}{\partial \varphi \partial r} - \frac{1}{r^2} \frac{\partial}{\partial \varphi} \right)
\end{aligned} \tag{8}$$

where ($b \leq a$)

$$\begin{aligned}
f_r(\varphi) &= \frac{\cos^2 \varphi}{a^2} + \frac{\sin^2 \varphi}{b^2} \\
f_\varphi(\varphi) &= \frac{\cos^2 \varphi}{b^2} + \frac{\sin^2 \varphi}{a^2} \\
f_{r\varphi}(\varphi) &= \left(\frac{1}{b^2} - \frac{1}{a^2} \right) \sin 2\varphi
\end{aligned} \tag{9}$$

We solve Laplace's equation using the basis of the circular problem. We consider the basis of states

$$\langle \vec{r} | kn \rangle = R_{kn} J_k(\gamma_{kn} r) e^{ik\varphi}. \tag{10}$$

The function J_k is the cylindrical Bessel function of order k , R_{kn} ensure that the basis is orthonormalized and γ_{kn} is the n zero of the Bessel function of order k . Imposing that

$$\begin{aligned}
\int_0^1 r dr \int_0^{2\pi} d\varphi R_{k'n'} J_{k'}(\gamma_{k'n'} r) e^{-ik'\varphi} R_{kn} J_k(\gamma_{kn} r) e^{ik\varphi} \\
= \delta_{k,k'} \delta_{n,n'}
\end{aligned}$$

we get that $R_{kn} = 1/(\sqrt{\pi} J_{k+1}(\gamma_{kn}))$.

In this basis the Hamiltonian of free electrons has the following matrix elements

$$\begin{aligned}
&\left(\frac{\hbar^2}{2ma^2\sigma^2} \right)^{-1} \langle k'n' | H_0 | kn \rangle = \\
&= \delta_{kk'} \delta_{nn'} \frac{1}{2} (\sigma^2 + 1) \gamma_{k'n'}^2 \\
&+ \delta_{k',k+2} \left(\frac{\pi}{2} (\sigma^2 - 1) \gamma_{k'-2,n}^2 \Gamma_{k'n';k'-2,n} \right. \\
&- \left. \pi (\sigma^2 - 1) \gamma_{k'-2,n} (k' - 1) \Lambda_{k'n';k'-2,n}^+ \right) \\
&+ \delta_{k',k-2} \left(\frac{\pi}{2} (\sigma^2 - 1) \gamma_{k'+2,n}^2 \Gamma_{k'n';k'+2,n} \right. \\
&- \left. \pi (\sigma^2 - 1) \gamma_{k'+2,n} (k' + 1) \Lambda_{k'n';k'+2,n}^- \right)
\end{aligned} \tag{11}$$

The following integrals are defined

$$\begin{aligned}
\Gamma_{k'n';k'-2,n} &= \int_0^1 r dr \frac{J_{k'}(\gamma_{k'n'}r)}{\sqrt{\pi}J_{k'+1}(\gamma_{k'n'})} \frac{J_{k'-2}(\gamma_{k'-2,n}r)}{\sqrt{\pi}J_{k'-1}(\gamma_{k'-2,n})} \\
\Gamma_{k'n';k'+2,n} &= \int_0^1 r dr \frac{J_{k'}(\gamma_{k'n'}r)}{\sqrt{\pi}J_{k'+1}(\gamma_{k'n'})} \frac{J_{k'+2}(\gamma_{k'+2,n}r)}{\sqrt{\pi}J_{k'+3}(\gamma_{k'+2,n})} \\
\Lambda_{k'n';k'-2,n}^+ &= \int_0^1 r dr \frac{J_{k'}(\gamma_{k'n'}r)}{\sqrt{\pi}J_{k'+1}(\gamma_{k'n'})} \frac{J_{k'-1}(\gamma_{k'-2,n}r)}{\sqrt{\pi}J_{k'-1}(\gamma_{k'-2,n})} \\
\Lambda_{k'n';k'+2,n}^- &= \int_0^1 r dr \frac{J_{k'}(\gamma_{k'n'}r)}{\sqrt{\pi}J_{k'+1}(\gamma_{k'n'})} \frac{J_{k'+1}(\gamma_{k'+2,n}r)}{\sqrt{\pi}J_{k'+3}(\gamma_{k'+2,n})}
\end{aligned} \tag{12}$$

For $k' = 0$ we get

$$\begin{aligned}
\Gamma_{0n';-2,n} &= - \int_0^1 r dr \frac{J_0(\gamma_{0n'}r)}{\sqrt{\pi}J_1(\gamma_{0n'})} \frac{J_2(\gamma_{2,n}r)}{\sqrt{\pi}J_1(\gamma_{2,n})} \\
\Lambda_{0n';-2,n}^+ &= \int_0^1 r dr \frac{J_0(\gamma_{0n'}r)}{\sqrt{\pi}J_1(\gamma_{0n'})} \frac{J_1(\gamma_{2,n}r)}{\sqrt{\pi}J_1(\gamma_{2,n})}
\end{aligned} \tag{13}$$

and for $k' = 1$ we get

$$\begin{aligned}
\Gamma_{1n';-1,n} &= - \int_0^1 r dr \frac{J_1(\gamma_{1n'}r)}{\sqrt{\pi}J_2(\gamma_{1n'})} \frac{J_1(\gamma_{1,n}r)}{\sqrt{\pi}J_0(\gamma_{1,n})} \\
\Lambda_{1n';-1,n}^+ &= \int_0^1 r dr \frac{J_1(\gamma_{1n'}r)}{\sqrt{\pi}J_2(\gamma_{1n'})} \frac{J_0(\gamma_{1,n}r)}{\sqrt{\pi}J_0(\gamma_{1,n})}
\end{aligned} \tag{14}$$

The various integrals have been calculated using Mathematica. The infinite set of terms has been truncated and the resulting finite matrix is diagonalized.

References

- [1] H.C. Manoharan, C.P. Lutz and D.M. Eigler, *Quantum mirages formed by coherent projection of electronic structure*, Nature **403**, 512 (2000), DOI: 10.1038/35000508.
- [2] G.A. Fiete and E.J. Heller, *Theory of quantum corrals and quantum mirages*, Rev. Mod. Phys. **75**, 933 (2003), DOI:https://doi.org/10.1103/RevModPhys.75.933.
- [3] D. Porras, J.F. Rossier and C. Tejedor, *Microscopic theory for quantum mirages in quantum corrals*, Phys. Rev. B **63**, 155406 (2001), DOI:https://doi.org/10.1103/PhysRevB.63.155406.
- [4] A.A. Aligia, *Many-body theory of the quantum mirage*, Phys. Rev. B **64**, 121102(R) (2001), DOI:https://doi.org/10.1103/PhysRevB.64.121102.

- [5] C. Trallero-Giner, S.E. Ulloa and V. López-Richard, *Local density of states in parabolic quantum corrals*, Phys. Rev. B **69**, 115423 (2004), DOI:<https://doi.org/10.1103/PhysRevB.69.115423>.
- [6] C. Trallero-Giner, V. López-Richard, S.E. Ulloa and G.E. Marques, *Eigenstate symmetries and information transfer in parabolic quantum reflectors*, Phys. Rev. B **79**, 153403 (2009), DOI:<https://doi.org/10.1103/PhysRevB.79.153403>.
- [7] O. Agam and A. Schiller, *Projecting the Kondo Effect: Theory of the Quantum Mirage*, Phys. Rev. Lett. **86**, 484 (2001), DOI:<https://doi.org/10.1103/PhysRevLett.86.484>.
- [8] V.S. Stepanyuk, L. Niebergall, W. Hergert and P. Bruno, *Ab initio Study of Mirages and Magnetic Interactions in Quantum Corrals*, Phys. Rev. Lett. **94**, 187201 (2005), DOI:<https://doi.org/10.1103/PhysRevLett.94.187201>.
- [9] E. Rossi and D.K. Morr, *Spatially Dependent Kondo Effect in Quantum Corrals*, Phys. Rev. Lett. **97**, 236602 (2006), DOI:<https://doi.org/10.1103/PhysRevLett.97.236602>.
- [10] M. Schmid and A.P. Kampf, *Mirages, anti-mirages, and further surprises in quantum corrals with non-magnetic impurities*, Ann. Phys. **12**, 463 (2003), DOI 10.1002/andp.200310023.
- [11] M. Schmid and A.P. Kampf, *Mirage phenomena in superconducting quantum corrals*, Ann. Phys. **14**, 556 (2005), DOI 10.1002/andp.200510058.
- [12] D.K. Morr and N.A. Stavropoulos, *Quantum Corrals, Eigenmodes, and Quantum Mirages in s-Wave Superconductors*, Phys. Rev. Lett. **92**, 107006 (2004), DOI:<https://doi.org/10.1103/PhysRevLett.92.107006>.
- [13] A. Lobos and A.A. Aligia, *One- and many-body effects on mirages in quantum corrals*, Phys. Rev. B **68**, 035411 (2003), DOI:<https://doi.org/10.1103/PhysRevB.68.035411>.
- [14] A.A. Aligia and A.M. Lobos, *Mirages and many-body effects in quantum corrals*, J. Phys. Cond. Matt. **17**, S1095 (2005), 10.1088/0953-8984/17/13/005/meta.
- [15] C.J. Bolech and E. Demler, *Observing Majorana bound States in p -Wave Superconductors Using Noise Measurements in Tunneling Experiments*, Phys. Rev. Lett. **98**, 237002 (2007), DOI:<https://doi.org/10.1103/PhysRevLett.98.237002>.
- [16] D.E. Liu and H.U. Baranger, *Detecting a Majorana-fermion zero mode using a quantum dot*, Phys. Rev. B **84**, 201308(R) (2011), DOI:<https://doi.org/10.1103/PhysRevB.84.201308>.
- [17] L. Fidkowski, J. Alicea, N.H. Lindner, R.M. Luscyn and M.P.A. Fisher, *Universal transport signatures of Majorana fermions in superconductor-Luttinger liquid junctions*, Phys. Rev. B **85**, 245121 (2012), DOI:<https://doi.org/10.1103/PhysRevB.85.245121>.
- [18] G.W. Semenoff and P. Sodano, *Stretched quantum states emerging from a Majorana medium*, J. Phys. B **40**, 1479 (2007), 10.1088/0953-4075/40/8/002/meta.
- [19] S. Tewari, C. Zhang, S. Das Sarma, C. Nayak and D.-H. Lee, *Testable Signatures of Quantum Nonlocality in a Two-Dimensional Chiral p -Wave Superconductor*, Phys. Rev. Lett. **100**, 027001 (2008), DOI:<https://doi.org/10.1103/PhysRevLett.100.027001>.

- [20] J. Nilsson, A.R. Akhmerov and C.W.J. Beenakker, *Splitting of a Cooper Pair by a Pair of Majorana Bound States*, Phys. Rev. Lett. **101**, 120403 (2008), DOI:<https://doi.org/10.1103/PhysRevLett.101.120403>.
- [21] K. Flensberg, *Non-Abelian Operations on Majorana Fermions via Single-Charge Control*, Phys. Rev. Lett. **106**, 090503 (2011), DOI:<https://doi.org/10.1103/PhysRevLett.106.090503>.
- [22] O. Brovko, P.A. Ignatiev and V.S. Stepanyuk, *Confined bulk states as a long-range sensor for impurities and a transfer channel for quantum information*, Phys. Rev. B **83**, 125415 (2011), DOI:<https://doi.org/10.1103/PhysRevB.83.125415>.
- [23] L. Fu, *Electron Teleportation via Majorana Bound States in a Mesoscopic Superconductor*, Phys. Rev. Lett. **104**, 056402 (2010), DOI:<https://doi.org/10.1103/PhysRevLett.104.056402>.
- [24] S. Vijay and L. Fu, *Teleportation-based quantum information processing with Majorana zero modes*, Phys. Rev. B **94**, 235446 (2016), DOI:<https://doi.org/10.1103/PhysRevB.94.235446>.
- [25] K. Michaeli, L. A. Landau, E. Sela and L. Fu, *Electron teleportation and statistical transmutation in multiterminal Majorana islands*, Phys. Rev. B **96**, 205403 (2017), DOI:<https://doi.org/10.1103/PhysRevB.96.205403>.
- [26] H.-M. Guo and M. Franz, *Theory of quasiparticle interference on the surface of a strong topological insulator*, Phys. Rev. B **81**, 041102(R) (2010), DOI:<https://doi.org/10.1103/PhysRevB.81.041102>.
- [27] Z. Su et al., *Mirage Andreev spectra generated by mesoscopic leads in nanowire quantum dots*, Phys. Rev. Lett. **121**, 127705 (2018), DOI:<https://doi.org/10.1103/PhysRevLett.121.127705>.
- [28] A. Yu. Kitaev, *Fault-tolerant quantum computation by anyons*, Annals of Phys. **303**, 2 (2003), [https://doi.org/10.1016/S0003-4916\(02\)00018-0](https://doi.org/10.1016/S0003-4916(02)00018-0).
- [29] C. Nayak, S. H. Simon, A. Stern, M. Freedman, and S. Das Sarma, *Non-Abelian anyons and topological quantum computation*, Rev. Mod. Phys. **80**, 1083 (2008), DOI:<https://doi.org/10.1103/RevModPhys.80.1083>.
- [30] J. Alicea, Y. Oreg, G. Refael, F. von Oppen, and M.P.A. Fisher, *Non-Abelian statistics and topological quantum information processing in 1D wire networks*, Nature Phys. **7**, 412 (2011), <https://doi.org/10.1038/nphys1915>.
- [31] F. Hassler, A.R. Akhmerov, and C.W.J. Beenakker, *The top-transmon: a hybrid superconducting qubit for parity-protected quantum computation*, New J. Phys. **13**, 095004 (2011), [10.1088/1367-2630/13/9/095004/meta](https://doi.org/10.1088/1367-2630/13/9/095004/meta).
- [32] J. Li, T. Neupert, B.A. Bernevig, *Manipulating Majorana zero modes on atomic rings with an external magnetic field*, Nat. Comm. **7**, 10395 (2016), <https://doi.org/10.1038/ncomms10395>.

- [33] B. Bauer, T. Karzig, R.V. Mishmash, A.E. Antipov and J. Alicea, *Dynamics of Majorana-based qubits operated with an array of tunable gates*, SciPost Phys. **5**, 004 (2018), doi: 10.21468/SciPostPhys.5.1.004.
- [34] C.-K. Chiu, M.M. Vazifeh, and M. Franz, *Majorana fermion exchange in strictly one-dimensional structures*, Europhys. Lett. **110**, 1001 (2015), doi: 10.1209/0295-5075/110/10001.
- [35] D. Rainis and D. Loss, *Majorana qubit decoherence by quasiparticle poisoning*, Phys. Rev. B **85**, 174533 (2012), DOI:<https://doi.org/10.1103/PhysRevB.85.174533>.
- [36] F.L. Pedrochi, D. P. DiVencenzo, *Majorana Braiding with Thermal Noise*, Phys. Rev. Lett. **115**, 120402 (2015), DOI:<https://doi.org/10.1103/PhysRevLett.115.120402>.
- [37] F.L. Pedrochi, N.E. Bonesteel, and D.P. DiVincenzo, *Monte Carlo studies of the self-correcting properties of the Majorana quantum error correction code under braiding*, Phys. Rev. B **92**, 115441 (2015), DOI:<https://doi.org/10.1103/PhysRevB.92.115441>.
- [38] N. Lang and H.P. Büchler, *Topological networks for quantum communication between distant qubits*, NPJ Quant. Inf. **3**, 47 (2017), <https://doi.org/10.1038/s41534-017-0047-x>.
- [39] L. Fu and C.L. Kane, *Superconducting Proximity Effect and Majorana Fermions at the Surface of a Topological Insulator*, Phys. Rev. Lett. **100**, 096407 (2008), DOI:<https://doi.org/10.1103/PhysRevLett.100.096407>.
- [40] R.M. Lutchyn, J.D. Sau and S. Das Sarma, *Majorana Fermions and a Topological Phase Transition in Semiconductor-Superconductor Heterostructures*, Phys. Rev. Lett. **105**, 077001 (2010), DOI:<https://doi.org/10.1103/PhysRevLett.105.077001>.
- [41] Y. Oreg, G. Refael and F. von Oppen, *Helical Liquids and Majorana Bound States in Quantum Wires*, Phys. Rev. Lett. **105**, 177002 (2010), DOI:<https://doi.org/10.1103/PhysRevLett.105.177002>.
- [42] S. Nadj-Perge, I.K. Drozdov, B.A. Bernevig and A. Yazdani, *Proposal for realizing Majorana fermions in chains of magnetic atoms on a superconductor*, Phys. Rev. B **88**, 020407 (2013), DOI:<https://doi.org/10.1103/PhysRevB.88.020407>.
- [43] S. Nadj-Perge, I.K. Drozdov, J. Li, H. Chen, S. Jeon, J. Seo, A.H. MacDonald, B.A. Bernevig and A. Yazdani, *Observation of Majorana fermions in ferromagnetic atomic chains on a superconductor*, Science **346**, 602 (2014), DOI: 10.1126/science.1259327.
- [44] Y. Peng, F. Pientka, L.I. Glazman and F. von Oppen, *Strong Localization of Majorana End States in Chains of Magnetic Atoms*, Phys. Rev. Lett. **114**, 106801 (2015), DOI:<https://doi.org/10.1103/PhysRevLett.114.106801>.
- [45] R. Pawlak, M. Kisiel, J. Klinovaja, T. Meier, S. Kawai, T. Glatzel, D. Loss, and E. Meyer, *Probing Atomic Structure and Majorana Wavefunctions in Mono-Atomic Fe-chains on Superconducting Pb-Surface*, npj Quant. Inf. **2**, 16035 (2016), <https://doi.org/10.1038/npjqi.2016.35>.

- [46] See for instance T. Čadež and P.D. Sacramento, *Zero energy modes in a superconductor with ferromagnetic adatom chains and quantum phase transitions*, J. Phys. Cond. Matt. **28**, 495703 (2016), and references therein, 10.1088/0953-8984/28/49/495703/meta.
- [47] K. Nakamura and H. Thomas, *Quantum Billiard in a Magnetic Field: Chaos and Diamagnetism*, Phys. Rev. Lett. **61**, 247 (1988), DOI:<https://doi.org/10.1103/PhysRevLett.61.247>.
- [48] The eigenstate chosen is level 34. Around this energy the spacing to the neighboring states is of the order of $6 - 7$ in the units of $\hbar^2 / (2ma^2\sigma^2) = 1$.